*M&C 2017 - International Conference on Mathematics & Computational Methods Applied to Nuclear Science & Engineering, Jeju, Korea, April 16-20, 2017, on USB (2017)*

**Discretization of Low-Order Quasidiffusion Equations on Arbitrary Quadrilaterals in 2D $r-z$ Geometry**

Jesse P. Jones,* Dmitriy Y. Anistratov,* Jim E. Morel,†

*Department of Nuclear Engineering, North Carolina State University, Raleigh, NC, United States
†Department of Nuclear Engineering, Texas A&M University, College Station, TX, United States
anistratov@ncsu.edu, jpjones6@ncsu.edu, morel@tamu.edu

**Abstract** - *We present a new discretization scheme for the low-order quasidiffusion (LOQD) equations in 2D $r-z$ geometry on arbitrary quadrilateral meshes. The second-order form of the LOQD equations is defined by the differential operator consisting of convection-diffusion with the Eddington tensor and extra operators with cross derivatives. The proposed discretization method is based on a second-order cell-centered scheme for the $P_1$ equations on arbitrary polygons. We conduct a study of the performance of this LOQD discretization scheme on a set of numerical tests with sequences of refined orthogonal and randomized grids. The numerical results show that the scheme converges with second order behavior.*

## I. INTRODUCTION

In this paper we present a discretization scheme for the low-order quasidiffusion (LOQD) equations in 2D $r-z$ geometry on spatial grids made up of arbitrary quadrilaterals. The quasidiffusion (QD) method is an efficient technique for solving transport problems [1, 2]. Not only do the iterations of the method converge rapidly, the QD method enables one to reduce the dimensionality of transport problems and improve coupling with multiphysics equations [3, 4]. The system of equations of the QD method consists of the high-order transport equation and the LOQD equations for the angular moments of the transport solution. Another feature of the QD method is that it is not necessary to discretize the high order and low order problems consistently in order to maintain iterative stability. Independent discretizations may be used. The second-order differential form of the LOQD equations has elements of a convection-diffusion equation with the Eddington tensor as well as some extra specific differential terms. These features of the differential LOQD equations require special discretization schemes.

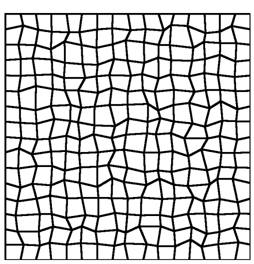

Fig. 1: Arbitrary quadrilateral grid under consideration.

In a wide class of transport problems the spatial mesh is defined by a different physical phenomenon. For instance, in problems stemming from high-energy density physics the radiative transfer equation is coupled with hydrodynamics. In cases such as this the spatial grid is determined by the hydrodynamic processes. These grids are often complex, and can change on each time step. In order to function in such multiphysics settings it is important for a computational method for solving radiative transfer problems to treat arbitrary meshes well.

Geometric models of spatial domains with rotational (axisymmetric) symmetry are described with 2D $r-z$ geometry. Such models arise in inertial confinement fusion, astrophysics, analysis of nuclear reactor concepts, etc. As in other curvilinear geometries, the streaming operator in $r-z$ geometry has certain unique features that represent challenges that one does not face in Cartesian geometry.

The remainder of this paper is organized as follows. In Sec. II we formulate the system of equations of the QD method in $r-z$ geometry. In Sec. III the discretization of the LOQD equations is derived. In Sec. IV we present numerical results demonstrating the convergence of the proposed discretization method when applied to the LOQD equations on sets of refined orthogonal and randomized quadrilateral meshes. Numerical results for diffusion problems are also shown. We conclude with a discussion in Sec. V.

## II. FORMULATION OF THE LOW-ORDER QD EQUATIONS IN $R-Z$ GEOMETRY

The steady-state, one-group transport equation in $r-z$ geometry takes the form

$$\frac{1}{r}\frac{\partial}{\partial r}\Big(r\Omega_r\psi\Big) + \frac{\partial}{\partial z}\Big(\Omega_z\psi\Big) + \frac{\partial}{\partial \gamma}\Big(\frac{1}{r}\Omega_\gamma\psi\Big) + \sigma_t\psi = \frac{1}{4\pi}(\sigma_s\phi + q)\,, \tag{1}$$

where the direction cosines are

$$\Omega_r = \sin\theta\cos\gamma\,, \quad \Omega_z = \cos\theta\,, \quad \Omega_\gamma = -\sin\theta\sin\gamma\,. \tag{2}$$

To derive the low-order QD equations for $\phi = \int_{4\pi}\psi d\boldsymbol{\Omega}$ and $\boldsymbol{J} = \int_{4\pi}\boldsymbol{\Omega}\psi d\boldsymbol{\Omega}$ we integrate the transport equation (1) over $\boldsymbol{\Omega}$ with weights 1, $\Omega_r$, and $\Omega_z$ to obtain

$$\frac{1}{r}\frac{\partial(rJ_r)}{\partial r} + \frac{\partial J_z}{\partial z} + \sigma_a\phi = q\,, \tag{3}$$

$$\frac{\partial F_{rr}}{\partial r} + \frac{\partial F_{zr}}{\partial z} + \frac{1}{r}\Big(2F_{rr} + F_{zz} - \phi\Big) + \sigma_t J_r = 0\,, \tag{4}$$

$$\frac{\partial F_{zr}}{\partial r} + \frac{\partial F_{zz}}{\partial z} + \frac{1}{r}F_{zr} + \sigma_t J_z = 0\,, \tag{5}$$

where $\sigma_a = \sigma_t - \sigma_s$, and

$$F_{\alpha\beta} = \int_{4\pi}\Omega_\alpha\Omega_\beta\psi d\boldsymbol{\Omega}\,, \quad \alpha,\beta = r,z\,. \tag{6}$$

The QD (aka Eddington) factors are defined as

$$E_{\alpha\beta} = \frac{\int_{4\pi} \Omega_\alpha \Omega_\beta \psi d\mathbf{\Omega}}{\int_{4\pi} \psi d\mathbf{\Omega}}\,, \quad \alpha,\beta = r,z\,. \tag{7}$$

We use the QD factors to formulate the first moment equations for $\phi$, $J_r$, and $J_z$. By also utilizing the fact that

$$E_{rr} + E_{zz} + E_{\gamma\gamma} = 1 \tag{8}$$

we obtain the first moment QD equations [3,5]

$$\frac{\partial(E_{rr}\phi)}{\partial r} + \frac{\partial(E_{zr}\phi)}{\partial z} + \frac{G}{r}E_{rr}\phi + \sigma_t J_r = 0\,, \tag{9}$$

$$\frac{1}{r}\frac{\partial(rE_{zr}\phi)}{\partial r} + \frac{\partial(E_{zz}\phi)}{\partial z} + \sigma_t J_z = 0\,, \tag{10}$$

where

$$G = 1 + \frac{E_{rr} + E_{zz} - 1}{E_{rr}}. \tag{11}$$

The system of equations of the QD method is defined by the high-order equation (1) and low-order equations (3), (9), and (10) with corresponding boundary conditions that relate the current and scalar flux to one another.

The iterative scheme of the QD method involves the solution of this two-level system of equations with the fixed-point iteration method. The transport equation (1) is solved to obtain the high-order transport solution which is used to compute the QD factors (7). These factors are then used as coefficients of the LOQD equations (3), (9) and (10). The LOQD equations are solved to get the low-order solution, namely, the angular moments $\phi$ and $\boldsymbol{J}$. The solution of the LOQD equations is then used to recompute source terms for the next iteration.

To simplify the derivation of a monotonic scheme for the LOQD equations, the first moment equation (9) is reformulated eliminating the non-differential term involving $\phi$. It is combined with the first differential term. We note that in general $G$ is a function of both $r$ and $z$. A reduced form of Eq. (9) is derived locally in each spatial cell of a given grid used in computations. Consider a spatial cell $C_i$, where $i$ is the cell index. We define the integrating factor

$$H_i(r,z) = \exp\left(\int_{r_i^*}^{r} \frac{G(r',z)}{r'}dr'\right), \quad \text{for} \quad r, r_i^*, z \in C_i \tag{12}$$

and multiply Eq. (9) by $H_i$ to obtain the aforementioned reduced form of the equation [6],

$$\frac{\partial(H_i E_{rr}\phi)}{\partial r} + H_i\frac{\partial(E_{zr}\phi)}{\partial z} + H_i\sigma_t J_r = 0\,. \tag{13}$$

This equation is used for the discretization of the LOQD equations in cell $C_i$. The integral within the exponential of $H_i$ can be approximated as

$$\int_{r_i^*}^{r} \frac{G(r',z)}{r'}dr' \approx \bar{G}_i \int_{r_i^*}^{r} \frac{1}{r'}dr' = \bar{G}_i \ln\left(\frac{r}{r_i^*}\right), \tag{14}$$

where

$$\bar{G}_i = \frac{1}{V_i}\int_{C_i} G(r,z) r dr dz\,, \tag{15}$$

and

$$V_i = \int_{C_i} r dr dz\,. \tag{16}$$

We use the following approximation of $\bar{G}_i$ in the cell $C_i$:

$$\bar{G}_i = 1 + \frac{\bar{E}_{rr,i} + \bar{E}_{zz,i} - 1}{\bar{E}_{rr,i}}\,, \tag{17}$$

where

$$\bar{E}_{\alpha\alpha,i} = \frac{1}{V_i}\int_{C_i} E_{\alpha\alpha}(r,z) r dr dz\,. \tag{18}$$

Inserting (14) into Eq. (12) yields

$$H_i = \left(\frac{r}{r_i^*}\right)^{\bar{G}_i} \quad \text{for} \quad r,z \in C_i\,. \tag{19}$$

Using Eq. (19) in Eq. (13) one gets

$$\frac{\partial(r^{\bar{G}_i}E_{rr}\phi)}{\partial r} + \frac{\partial(r^{\bar{G}_i}E_{zr}\phi)}{\partial z} + r^{\bar{G}_i}\sigma_t J_r = 0 \quad \text{for} \quad r,z \in C_i\,. \tag{20}$$

As a result, in the spatial cell $C_i$ the LOQD equations have the form

$$\frac{1}{r}\frac{\partial(rJ_r)}{\partial r} + \frac{\partial J_z}{\partial z} + \sigma_a\phi = q\,, \tag{21a}$$

$$\frac{1}{r^{\bar{G}_i}}\frac{\partial(r^{\bar{G}_i}E_{rr}\phi)}{\partial r} + \frac{\partial(E_{zr}\phi)}{\partial z} + \sigma_t J_r = 0\,, \tag{21b}$$

$$\frac{1}{r}\frac{\partial(rE_{zr}\phi)}{\partial r} + \frac{\partial(E_{zz}\phi)}{\partial z} + \sigma_t J_z = 0\,. \tag{21c}$$

In general the boundary conditions of the LOQD equations in $r-z$ are mixed (Robin) boundary conditions for $\phi$ and the normal components of $\boldsymbol{J}$ defined with QD boundary factors [7,8]. There is a symmetry boundary condition at r=0 that is equivalent to a reflective BC.

The LOQD equations reduce to the diffusion equations in $P_1$ form when

$$E_{rr} = E_{zz} = \frac{1}{3}\,, \tag{22a}$$

$$E_{zr} = 0\,. \tag{22b}$$

These values for the Eddington tensor cause the factor $G$ to be zero. The $P_1$ equations in $r-z$ geometry are given by

$$\frac{1}{r}\frac{\partial(rJ_r)}{\partial r} + \frac{\partial J_z}{\partial z} + \sigma_a\phi = q\,, \tag{23a}$$

$$\frac{1}{3}\frac{\partial\phi}{\partial r} + \sigma_t J_r = 0\,, \tag{23b}$$

$$\frac{1}{3}\frac{\partial\phi}{\partial z} + \sigma_t J_z = 0\,. \tag{23c}$$

## III. DISCRETIZATION OF LOQD EQUATIONS

The general form of the LOQD equations is

$$\boldsymbol{\nabla} \cdot \boldsymbol{J} + \sigma_a \phi = q \,, \tag{24a}$$

$$\boldsymbol{J} = -\frac{1}{\sigma_t} \nabla \cdot (\mathbb{E}\phi) \,, \tag{24b}$$

where $\mathbb{E}$ is the QD (Eddington) tensor. In $r-z$ geometry we have

$$\nabla_r = \frac{1}{r}\frac{\partial}{\partial r} \,, \quad \nabla_z = \frac{\partial}{\partial z} \,. \tag{25}$$

Equation (24b) shows that discretization of the LOQD equations in this first-order form involves the definition of an approximation for tensor divergence. The discretization that we propose for the LOQD equations in $r-z$ is based on a cell-centered scheme for the $P_1$ equations on arbitrary polygons and a scheme for the LOQD equations in 2D $x-y$ geometry [9, 10].

We approximate the LOQD equations (21) locally in each cell. The unknowns in $C_i$ are

1. the cell-average scalar fluxes $\phi_{i,c}$,
2. the face-average scalar fluxes $\phi_{i,f}$,
3. the normal components of face-average currents $J_{i,f} = \boldsymbol{n}_{i,f} \cdot \boldsymbol{J}_{i,f}$, where $\boldsymbol{n}_{i,f} = (n^r_{i,f}, n^z_{i,f})$ is the outward normal of face $f$ of cell $i$.

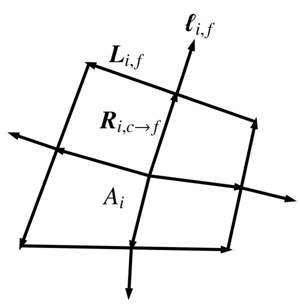


Fig. 2: Definition of arbitrary cell.

We integrate the balance equation (21a) over the cell $C_i$ to get

$$\sum_{f\in C_i} A_{i,f} J_{i,f} + \sigma_{a,i}\phi_{i,c} V_i = Q_i V_i \,, \tag{26}$$

where $A_{i,f}$ is the face area. The first moment equations are approximated at cell faces as

$$n^r_{i,f}\left(\frac{1}{r^{\bar{G}_i}}\frac{\partial(r^{\bar{G}_i}E_{rr}\phi)}{\partial r} + \frac{\partial(E_{zr}\phi)}{\partial z}\right)\Bigg|_{i,f} + n^z_{i,f}\left(\frac{1}{r}\frac{\partial(rE_{zr}\phi)}{\partial r} + \frac{\partial(E_{zz}\phi)}{\partial z}\right)\Bigg|_{i,f} + \sigma_{t,i}J_{i,f} = 0 \,. \tag{27}$$

To derive the discretization of the tensor divergence terms at cell faces in Eq. (27) we apply the cell-face approximation of the gradient of the scalar flux used in the cell-centered diffusion discretization proposed in [9]. This approach enabled the derivation of an accurate 2nd-order cell-local discretization of the LOQD equations in 2D Cartesian geometry on arbitrary quadrilateral meshes [10]. The proposed approximation of the gradient in $r-z$ geometry is given by

$$\boldsymbol{\nabla}\phi_{i,f} = (\phi_{i,f} - \phi_{i,c})\boldsymbol{\xi}_{i,f} + \frac{1}{A_i}\sum_{f'\neq f}\phi_{i,f'}\boldsymbol{\eta}_{i,f',f} \,, \tag{28}$$

where

$$\boldsymbol{\xi}_{i,f} = \frac{\boldsymbol{\ell}_{i,f}}{\boldsymbol{R}_{i,c\to f}\cdot\boldsymbol{\ell}_{i,f}} \,, \tag{29}$$

$$\boldsymbol{\eta}_{i,f',f} = \boldsymbol{\ell}_{i,f'} - \frac{\boldsymbol{R}_{i,c\to f}\cdot\boldsymbol{\ell}_{i,f'}}{\boldsymbol{R}_{i,c\to f}\cdot\boldsymbol{\ell}_{i,f}}\boldsymbol{\ell}_{i,f} \,, \tag{30}$$

$$\boldsymbol{\ell}_{i,f} = \boldsymbol{n}_{i,f}\|\boldsymbol{L}_{i,f}\|, \,, \tag{31}$$

$$A_i = \int_{C_i} drdz \,, \tag{32}$$

$$\boldsymbol{R}_{i,c\to f} = \boldsymbol{r}_{i,c} - \boldsymbol{r}_{i,f} \,. \tag{33}$$

As shown in Figure 2, $\boldsymbol{L}_{i,f}$ is the vector that goes between two adjacent corners of a cell. $\boldsymbol{r}_{i,f}$ is the coordinate vector of the face center, and $\boldsymbol{r}_{i,c}$ is the coordinate vector of the cell centroid. The cell centroid is defined to be the volume centroid of the 3D volume of $C_i$. We note that in this discretization we use area averaging for the gradient over a cell

$$\langle\boldsymbol{\nabla}\phi\rangle_i = \frac{1}{A_i}\int_{C_i}\boldsymbol{\nabla}\phi drdz = \frac{1}{A_i}\sum_{f\in C_i}\phi_{i,f}\boldsymbol{\ell}_{i,f} \,. \tag{34}$$

This choice of averaging leads to a second-order approximation and preservation of spherical symmetry [11]. This form of the average gradient is uniform in $\gamma$, i.e. it applies throughout a cell's entire volume in 3D.

We apply the discretization of the gradient on a cell face (28) to the derivative terms in (27) in the following way:

$$\left\{\frac{\partial g}{\partial r}\right\}_{i,f} = \boldsymbol{e}_r \cdot \{\boldsymbol{\nabla} g\}_{i,f} \,, \tag{35a}$$

$$\left\{\frac{\partial g}{\partial z}\right\}_{i,f} = \boldsymbol{e}_z \cdot \{\boldsymbol{\nabla} g\}_{i,f} \,, \tag{35b}$$

where $g$ is a scalar function, for example, $rE_{rz}\phi$, $E_{zz}\phi$ etc. As a result we obtain the approximation of the first-moment equation at cell faces given by

$$\begin{aligned}
& n^r_{i,f}\Bigg[\frac{1}{r^{\bar{G}_i}{}_{i,f}}\Bigg(\Big(r^{\bar{G}_i}_{i,f}E_{rr,i,f}\phi_{i,f} - r^{\bar{G}_i}_{i,c}E_{rr,i,c}\phi_{i,c}\Big)\boldsymbol{\xi}_{i,f}\cdot\boldsymbol{e}_r \\
&\qquad + \frac{1}{A_i}\sum_{f'\neq f} r^{\bar{G}_i}_{i,f'}E_{rr,i,f'}\phi_{i,f'}\boldsymbol{\eta}_{i,f',f}\cdot\boldsymbol{e}_r\Bigg) \\
& + \Big(E_{rz,i,f}\phi_{i,f} - E_{rz,i,c}\phi_{i,c}\Big)\boldsymbol{\xi}_{i,f}\cdot\boldsymbol{e}_z + \frac{1}{A_i}\sum_{f'\neq f}E_{rz,i,f'}\phi_{i,f'}\boldsymbol{\eta}_{i,f',f}\cdot\boldsymbol{e}_z\Bigg] \\
&\quad + n^z_{i,f}\Bigg[\frac{1}{r_{i,f}}\Bigg(\Big(r_{i,f}E_{rz,i,f}\phi_{i,f} - r_{i,c}E_{rz,i,c}\phi_{i,c}\Big)\boldsymbol{\xi}_{i,f}\cdot\boldsymbol{e}_r \\
&\qquad + \frac{1}{A_i}\sum_{f'\neq f} r_{i,f'}E_{rz,i,f'}\phi_{i,f'}\boldsymbol{\eta}_{i,f',f}\cdot\boldsymbol{e}_r\Bigg) + \\
& \Big(E_{zz,i,f}\phi_{i,f} - E_{zz,i,c}\phi_{i,c}\Big)\boldsymbol{\xi}_{i,f}\cdot\boldsymbol{e}_z + \frac{1}{A_i}\sum_{f'\neq f}E_{zz,i,f'}\phi_{i,f'}\boldsymbol{\eta}_{i,f',f}\cdot\boldsymbol{e}_z\Bigg] \\
&\qquad + \sigma_{t,i}\boldsymbol{n}_{i,f}\cdot\boldsymbol{J}_{i,f} = 0
\end{aligned} \tag{36}$$

Consequentially the proposed discretization of the LOQD equations in $r-z$ geometry is defined by Eqs. (26) and (36).

## IV. RESULTS AND ANALYSIS

We performed a number of tests to evaluate the performance of the developed scheme when applied to the diffusion equation as well as the LOQD equations with prescribed analytic factors. The tests we present here were selected to analyze the convergence of the method on both orthogonal and arbitrary grids. The arbitrary grids used were created by perturbing the quadrilateral vertexes of originally orthogonal grids. The perturbation of each vertex is done in a random direction and with a random magnitude between zero and a specified percent of the grid spacing. Unless otherwise stated, the maximum perturbation used was 35% as this is very near the limit where concave quadrilaterals can result.

### 1. Test 1: Diffusion with linear solution in z

The first test we present is for a diffusion problem. The proposed method is of second order, and as a result we expect exact treatment of problems with linear solutions. This test is meant to show that the method reproduces linear solutions on randomized grids. The domain of this test is $r \in [0, 1]$, $z \in [0, 1]$. For this problem there is no external source, and the cross sections are taken to be $\sigma_t = \sigma_s = 1$ [12]. The left boundary is on the rotational axis and hence

$$\boldsymbol{n} \cdot \boldsymbol{J}|_{r=0} = 0\,, \quad \text{for} \quad z \in [0, 1]\,. \tag{37a}$$

The right boundary is taken to be reflective,

$$\boldsymbol{n} \cdot \boldsymbol{J}|_{r=1} = 0\,, \quad \text{for} \quad z \in [0, 1]\,. \tag{37b}$$

The condition at the top is defined to be a Marshak vacuum boundary,

$$\boldsymbol{n} \cdot \boldsymbol{J}|_{z=1} = \frac{1}{2}\phi\,, \quad \text{for} \quad r \in [0, 1]\,. \tag{37c}$$

The bottom boundary with incoming radiation is given by

$$\boldsymbol{n} \cdot \boldsymbol{J}|_{z=0} = \frac{1}{2}\phi + 1\,, \quad \text{for} \quad r \in [0, 1]\,. \tag{37d}$$

The solution of this diffusion problem is linear in $z$.

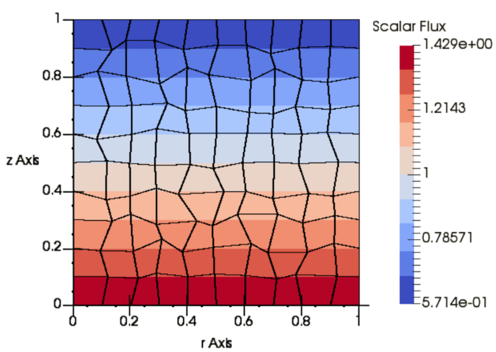


Fig. 3: Isoline graph with computational mesh.

Figure 3 shows the result as well as the computational grid used for the problem. We chose to use a coarse color map for the solution to act as an isoline plot to highlight the linear solution the proposed scheme obtains throughout the domain. The magnitude as well as the slope matches the analytic solution with high accuracy even for this coarse mesh. The norm of the difference between the numerical solution and analytic solution is on the order of the convergence criterion used for solving the equations:

$$||\phi - \phi^*||_2 = 2.7219 \times 10^{-14}\,. \tag{38}$$

This confirms that the method reproduces linear solutions.

### 2. Test 2: Convergence study for the proposed scheme applied to diffusion problems

The second set of results is a grid refinement convergence study of the method when applied to the $P_1$ equations. For this test case we ran a problem with a series of grids each refined by a factor of two. We use Aitken extrapolation to generate a reference value based on the solutions computed specifically on the sequence of orthogonal grids. This reference value was then used to determine the convergence order of the scheme on the orthogonal as well as the arbitrary grids.

Being a diffusion problem, the diagonal of the QD (Eddington) tensor is set to one third, and the off diagonal terms become zero ($E_{rr}$=$E_{zz}$=$\frac{1}{3}$, $E_{zr}$=0) as pointed out earlier. The domain of the problem is 1.0 cm × 1.0 cm. The medium is homogeneous with cross sections $\sigma_t = \sigma_a = 1.0$, and a uniform external source $q = 1.0$. The boundary conditions are vacuum at every side of the problem domain defined by the Marshak BCs (see Eq. (37c)). Table I shows the integral of the scalar flux over the problem domain $\Phi = \int_D \phi(r, z) r dr dz$ and the estimated order of convergence $P$ for each grid used. The subscripts on $\Phi$ and $P$ indicate the maximum perturbation of the vertexes used for generating the grid. Figure 4 demonstrates convergence of the scheme with mesh refinement. These results show that the method does converge with second order accuracy for diffusion problems.

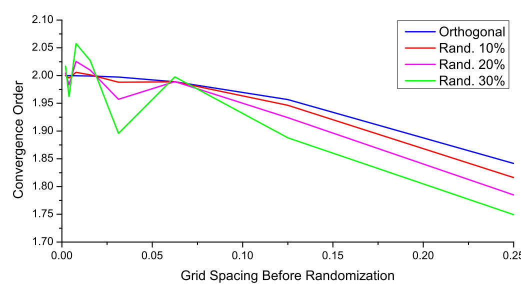


Fig. 4: Order of spatial convergence ($P$) for the diffusion problem in Test 2.

### 3. Test 3: Two region diffusion problem

The next test we performed is a diffusion problem devised to demonstrate the convergence of the solution obtained by the scheme on successively refined randomized grids throughout space. The test consists of a homogeneous medium with cross sections $\sigma_t = 1.0, \sigma_s = 0.5$. The domain of the problem is $r \in [0, 5], z \in [0, 3]$. The left half of the domain has a unit

TABLE I: Convergence study of proposed scheme applied to the diffusion equation.

| Grid | $\Phi_{ortho}$ | $P_{ortho}$ | $\Phi_{10\%}$ | $P_{10\%}$ | $\Phi_{20\%}$ | $P_{20\%}$ | $\Phi_{30\%}$ | $P_{30\%}$ |
|---|---|---|---|---|---|---|---|---|
| $2 \times 2$ | 1.278075 | - | 1.277001 | - | 1.275963 | - | 1.274953 | - |
| $4 \times 4$ | 1.236202 | 1.841716 | 1.236187 | 1.816122 | 1.236240 | 1.784914 | 1.236345 | 1.749356 |
| $8 \times 8$ | 1.224173 | 1.956789 | 1.224200 | 1.946467 | 1.224279 | 1.924215 | 1.224417 | 1.887710 |
| $16 \times 16$ | 1.221051 | 1.988968 | 1.221058 | 1.988892 | 1.221078 | 1.989076 | 1.221106 | 1.997645 |
| $32 \times 132$ | 1.220263 | 1.997238 | 1.220267 | 1.988105 | 1.220277 | 1.957413 | 1.220297 | 1.895649 |
| $64 \times 64$ | 1.220065 | 1.999311 | 1.220067 | 2.001336 | 1.220069 | 2.009691 | 1.220073 | 2.027179 |
| $128 \times 128$ | 1.220016 | 1.999827 | 1.220016 | 2.005964 | 1.220017 | 2.025359 | 1.220017 | 2.057445 |
| $256 \times 256$ | 1.220004 | 1.999948 | 1.220004 | 1.995849 | 1.220004 | 1.982960 | 1.220004 | 1.962297 |
| $512 \times 512$ | 1.220001 | 1.999899 | 1.220001 | 2.000253 | 1.220001 | 2.004501 | 1.220001 | 2.016958 |
| Reference | 1.219999906 | | | | | | | |

external source, while the right side has no source. This test has two individual cases that both have two randomized sub domains separated by an orthogonal line of cell boundaries. The first test has a straight vertical line of faces at the problem midpoint, $r = 2.5$, refer to Figure 5. The second test is identical except that the line of straight faces is horizontal at the problem midpoint, namely $z = 1.5$. The results for this

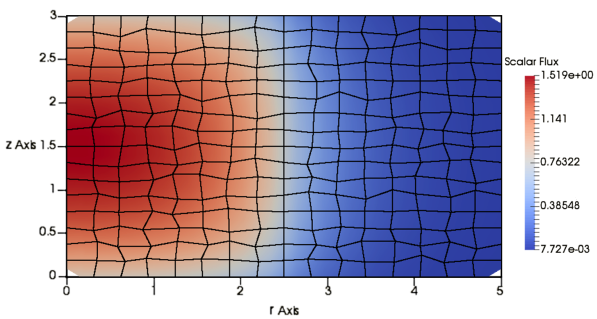


Fig. 5: Scalar flux solution on two region randomized grid.

test are cross sectional slices of the solution running through the non-randomized cell edges for both cases. This allows for demonstration of the point wise behavior of the solution as the grid is refined. We give the solution for both cases on five grids as indicated in Figures 6 and 7. These results show that upon refinement the solution on randomized grids converges to the solution obtained on a fine orthogonal grid point wise.

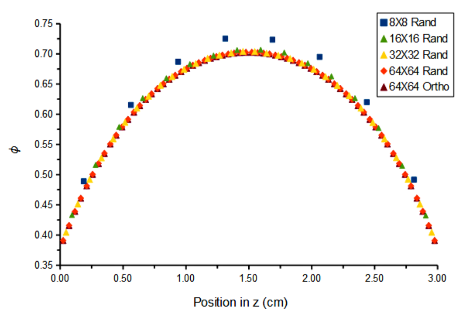


Fig. 6: Test 3, case 1: $\phi(2.5, z)$.

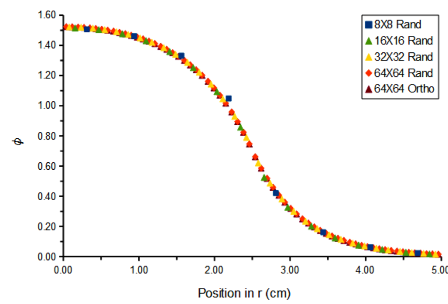


Fig. 7: Test 3, case 2: $\phi(r, 1.5)$.

## 4. Test 4: Convergence study for the proposed scheme applied to the LOQD equations

The fourth and final set of results is a grid refinement convergence study conducted to asses the convergence order of the scheme for discretization of the LOQD equations. This test uses the same methodology as Test 2, as well as the same problem domain, grids, source, and cross sections. The QD factors for this problem are given by the following functions:

$$E_{rr}(r,z) = E_{zz}(r,z) = \frac{1}{3} + r(z - 0.5H)^2 , \tag{39a}$$

$$E_{zr}(r,z) = r(z - 0.5H) . \tag{39b}$$

The result are shown in Table II and Figure 8. They demonstrate that the scheme for the LOQD equations has second order convergence.

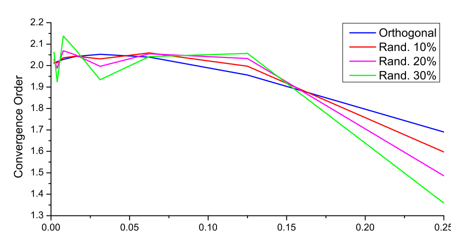


Fig. 8: Order of convergence of the scheme for the LOQD equations in Test 4.

TABLE II: Convergence study of the scheme for the LOQD equations.

| Grid | $\Phi_{ortho}$ | $P_{ortho}$ | $\Phi_{10\%}$ | $P_{10\%}$ | $\Phi_{20\%}$ | $P_{20\%}$ | $\Phi_{30\%}$ | $P_{30\%}$ |
|---|---|---|---|---|---|---|---|---|
| $2\times2$ | 2.208801 | - | 2.207309 | - | 2.205604 | - | 2.203537 | - |
| $4\times4$ | 2.150528 | 1.690193 | 2.151779 | 1.597145 | 2.153356 | 1.486457 | 2.155228 | 1.359026 |
| $8\times8$ | 2.131107 | 1.955894 | 2.131230 | 1.997202 | 2.131447 | 2.032905 | 2.131780 | 2.056843 |
| $16\times16$ | 2.126003 | 2.039600 | 2.126010 | 2.059165 | 2.126067 | 2.054738 | 2.126164 | 2.041799 |
| $32\times132$ | 2.124758 | 2.052664 | 2.124765 | 2.030835 | 2.124789 | 1.996692 | 2.124834 | 1.933787 |
| $64\times64$ | 2.124458 | 2.042435 | 2.124460 | 2.043740 | 2.124465 | 2.049676 | 2.124474 | 2.073888 |
| $128\times128$ | 2.124386 | 2.028681 | 2.124386 | 2.036530 | 2.124387 | 2.069303 | 2.124388 | 2.137791 |
| $256\times256$ | 2.124368 | 2.017945 | 2.124368 | 2.012682 | 2.124368 | 1.987575 | 2.124369 | 1.924366 |
| $512\times512$ | 2.124364 | 2.011505 | 2.124364 | 2.014204 | 2.124364 | 2.028482 | 2.124364 | 2.062315 |
| Reference | 2.124362129 | | | | | | | |

## V. CONCLUSIONS

We developed a new discretization method for the low-order quasidiffusion equations in $r-z$ geometry for arbitrary quadrilateral meshes. The developed discretization is 2nd order in space on arbitrary grids of quadrilaterals. Numerical results showed that the method is both stable and converges with 2nd order behavior on a sequence of refined randomized grids. In future work this discretization method will be extended to adaptive like grids with cells having multiple neighbors across a face. We will also proceed with developing the QD method for transport problems in $r-z$ geometry based on this discretization of the LOQD equations.

## ACKNOWLEDGMENTS

Work by the first author (JPJ) was supported by a graduate fellowship from the Nuclear Engineering University Program (NEUP) of the U.S. Department of Energy.

## REFERENCES

1. V. YA. GOL'DIN, "A Quasi-Diffusion Method of Solving the Kinetic Equation," *USSR Comp. Math. and Math. Phys.*, **4**, 136–149 (1964).
2. M. L. ADAMS and E. W. LARSEN, "Fast Iterative Methods for Discrete-Ordinates Particle Transport Calculations," *Progress in Nuclear Energy*, **40**, 3–159 (2002).
3. E. N. ARISTOVA, V. YA. GOL'DIN, and A. V. KOLPAKOV, "Multidimensional Calculations of Radiation Transport by Nonlinear Quasi-Diffusion Method," in "Proceedings of Int. Conf. on Math. and Comp., M&C 1999," (1999), pp. 667–676, Madrid, Spain, October 7-10.
4. A. TAMANG and D. Y. ANISTRATOV, "A Multilevel Projective Method for Solving the Space-Time Multigroup Neutron Kinetics Equations Coupled with the Heat Transfer Equation," *Nuclear Science and Engineering*, **177**, 1–18 (2014).
5. E. N. ARISTOVA, "Simulation of Radiation Transport in a Channel Based on the Quasi-Diffusion Method," *Transp. Theory and Stat. Phys.*, **37**, 483–503 (2008).
6. D. Y. ANISTRATOV and V. YA. GOL'DIN, "Nonlinear Methods for Solving Particle Transport Problems," *Transp. Theory and Stat. Phys.*, **22**, 42–77 (1993).
7. V. YA. GOL'DIN and B. N. CHETVERUSHKIN, "Methods of Solving One-Dimensional Problems of Radiation Gas Dynamics," *USSR Comp. Math. and Math. Phys.*, **12**, 177–189 (1972).
8. M. M. MIFTEN and E. W. LARSEN, "The Quasi-Diffusion Method for Solving Transport Problems in Planar and Spherical Geometries," *Transport Theory Statist. Phys.*, **22**, 165–186 (1993).
9. J. E. MOREL, "A 3-D Cell-Centered Diffusion Discretization for Arbitrary Polyhedral Meshes," Tech. rep., Los Alamos National Laboratory (2002), LANL Research Note, CCS-4:02-40(U).
10. W. A. WIESELQUIST, D. Y. ANISTRATOV, and J. E. MOREL, "A Cell-Local Finite Difference Discretization of the Low-Order Quasidiffusion Equations for Neutral Particle Transport on Unstructured Quadrilateral Meshes," *J. Comp. Phys.*, **273**, 343–357 (2014).
11. T. S. PALMER, "Discretizing the Diffusion Equation on Unstructured Polygonal Meshes in Two Dimensions," *Annals of Nuclear Energy*, **28**, 1851–1880 (2001).
12. J. E. MOREL, R. M. ROBERTS, and M. J. SHASHKOV, "A Local Support-Operators Diffusion Discretization Scheme for Quadrilateral r-z Meshes," *Journal of Computational Physics*, **144**, 17–51 (1997).